Anal. Chem. 1994, *66*, 692–698

Effects of Cations and Charge Types on the Metastable Decay Rates of Oligosaccharides

Lambert C. Ngoka,† Jean-François Gal,‡ and Carlito B. Lebrilla*,†

Department of Chemistry, University of California, Davis, California 95616, and Groupe FT-ICR, Université de Nice-Sophia Antipolis, 06108 Nice Cedex 2, France

Metastable decay rates of α-cyclodextrin and maltohexaose coordinated to proton and alkali metal ions were determined from ions produced by liquid secondary ion mass spectrometry in an external source Fourier transform mass spectrometry instrument. For both oligosaccharide compounds the decay rates of the protonated species are faster than any alkali metal coordinated species. Decay rates of the metal cationized species decrease in the order Li^+, Na^+, K^+, and Cs^+. The anion of α-cyclodextrin has the slowest measurable decomposition rate. The relationships between cation affinities and rates are explored.

The progress in multiple or tandem mass spectrometry (MS) techniques has been driven, in large part, by the need to obtain more structurally important fragment ions.[1] Despite the often violent processes involved in ionization, adequate energy for producing fragment ions is often not attained. In addition, as the analyses are increasingly performed with larger molecules, there is concern that the degree of fragmentation will further decrease. Several theories predict that instead of becoming more susceptible to fragmentation, molecules become more resistant to fragmentation due to the greater number of states available to distribute the energy.[2-5]

The study of the unimolecular decay of large polyfunctional molecules is important for understanding the dynamics of fragmentation. Several investigations on metastable decay have been performed primarily on small molecules (<20 atoms) with mass spectrometers, particularly sector and time of flight instruments, that have time scales equivalent to the rate of the processes.[6-16] More recently, metastable decompositions of biomolecules have been reported which extend beyond the time scales of these techniques.[9,17] Fourier transform mass spectrometry (FTMS) has advantages in these slow processes as the detection delay time is variable, ranging from milliseconds to minutes. In a recent publication, we described the metastable decomposition of protonated α-cyclodextrin produced by liquid secondary ion mass spectrometry (LSIMS) with an external source FTMS instrument. The observed rate of $4.2 \times 10^2\ s^{-1}$ is to our knowledge the slowest decay rate for an ionic species produced from direct ionization.[18]

In this report, we investigate the role of the cationizing atom and the charge type on metastable decomposition of α-cyclodextrin and maltohexaose. Oligosaccharides have been chosen due to our research group's general interest in this class of compounds and to the problems often associated with their analyses, specifically poor sensitivity and the lack of structurally important fragment ions.[19-25] Doping the sample with alkali metal salts has been reported to increase the sensitivity by producing a greater abundance of pseudomolecular ions.[21,26] Additionally, it has been shown that fragmentation products differ, depending on the coordinating cation and on the charge (anion or cation) of the species.[27,28] For example, protonated oligosaccharides produce primarily cleavage along the glycosidic bonds while both lithiated and deprotonated oligosaccharides fragment to also produce cross ring cleavages. It would also be appropriate and highly desirable to study the effects of size on the rates of metastable decay. However, these investigations may be complicated by mass-dependent ion loss processes that operate in all ion trapping MS methods. In the FTMS, these processes can occur over a large mass range and may complicate comparisons between metastable decay rates of large (>1000 amu) and small (<500 amu) ionic species.

† University of California.
‡ Université de Nice-Sophia Antipolis.

(1) *Tandem Mass Spectrometry*; McLafferty, F. W., Ed.; John Wiley and Sons: New York, 1983.
(2) Craig, A.; Derrick, P. *J. Am. Chem. Soc.* **1985**, *107*, 6707.
(3) King, B.; Ziv, A.; Lin, S.; Tsong, I. *J. Chem. Phys.* **1985**, *82*, 3641.
(4) Bunker, D. L.; Wang, F.-M. *J. Am. Chem. Soc.* **1977**, *99*, 7457.
(5) Griffin, L. L.; McAdoo, D. J. *J. Am. Soc. Mass Spectrom.* **1993**, *4*, 11.
(6) Bensimon, M.; Rapin, J.; Gaumann, T. *Int. J. Mass Spectrom. Ion Processes* **1986**, *72*, 125.
(7) Beckey, H. D.; Hey, H.; Levsen, K.; Tenschert, G. *Int. J. Mass Spectrom. Ion Phys.* **1969**, *2*, 101.
(8) Beynon, J. H.; Fontaine, A. E.; Lester, G. R. *Int. J. Mass Spectrom. Ion Phys.* **1972**, *8*, 341.
(9) Demirev, P.; Olthoff, J. K.; Fenselau, C.; Cotter, R. J. *Anal. Chem.* **1987**, *59*, 1951.
(10) Futrell, J. H.; Stephan, K.; Märk, T. D. *J. Chem. Phys.* **1982**, *76*, 5893.
(11) Hills, L. P.; Futrell, J. H. *Org. Mass Spectrom.* **1972**, *5*, 1019.
(12) Huntress, W. T. J.; Sen, S. D. K.; Jennings, K. R.; Bowers, M. T. *Int. J. Mass Spectrom. Ion Phys.* **1977**, *24*, 25.
(13) Kim, Y. H.; Kim, M. S. *Rapid Commun. Mass Spectrom.* **1991**, *5*, 25.
(14) Kühlewind, H.; Neusser, H. J.; Schlag, E. W. *Int. J. Mass Spectrom. Ion Phys* **1983**, *51*, 255.
(15) Kühlewind, H.; Neusser, H. J.; Schlag, E. W. *J. Phys. Chem.* **1984**, *88*, 6104.
(16) Neusser, H. J.; Kühlewind, H.; Boesl, U.; Schlag, E. W. *Ber. Bunsen-Ges. Phys. Chem.* **1985**, *89*, 276.
(17) Schueler, B.; Beavis, R.; Ens, W.; Main, D. E.; Tang, X.; Standing, K. G. *Int. J. Mass Spectrom. Ion Processes* **1989**, *92*, 185.
(18) Ngoka, L.; Lebrilla, C. B. *J. Am. Soc. Mass Spectrom.* **1993**, *4*, 210.
(19) Dell, A.; Oates, J. E.; Morris, H. R.; Egge, H. *Int. J. Mass Spectrom. Ion Phys.* **1983**, *46*, 415.
(20) Dell, A.; Morris, H. R.; Egge, H.; Nicolai, H. V.; Strecker, G. *Carbohydr. Res.* **1983**, *115*, 41.
(21) Dell, A. *Adv. Carbohydr. Chem. Biochem.* **1987**, *45*, 19.
(22) Carr, S. A.; Reinhold, V. N.; Green, B. N.; Hass, J. R. *Biomed. Mass Spectrom.* **1985**, *12*, 288.
(23) Reinhold, V. N.; Carr, S. A. *Mass Spectrom. Rev.* **1983**, *2*, 153.
(24) Biemann, K. In *Methods in Enzymology*; McCloskey, J. A., Ed.; Academic Press: San Diego, CA, 1990; Vol. 193.
(25) Carroll, J. A.; Ngoka, L.; McCullough, S. M.; Gard, E.; Jones, A. D.; Lebrilla, C. B. *Anal. Chem.* **1991**, *63*, 2526.
(26) Puzo, G.; Prome, J. C. *Org. Mass Spectrom.* **1984**, *19*, 448.
(27) Zhou, Z.; Ogden, S.; Leary, J. A. *J. Org. Chem.* **1990**, *55*, 5444.
(28) Hofmeister, G. E.; Zhou, Z.; Leary, J. A. *J. Am. Chem. Soc.* **1991**, *113*, 5964.

0003-2700/94/0366-0692$04.50/0

EXPERIMENTAL SECTION

An external source FTMS instrument, equipped with a quadrupole ion guide and a 3-T magnet, was used. Detailed descriptions of the instrument are provided in earlier publications.[25,29] The Omega data system (IonSpec Corp.) controls the pulse sequence and data acquisition of the instrument. Ions were created by a liquid secondary ion mass spectrometry (LSIMS) source with a Cs^+ primary beam. Protonated and deprotonated species were produced by dissolving the compound in deionized water and placing a 2-μL aliquot on the sample probe in either a pure glycerol or a glycerol/thioglycerol (1:1 mixture) matrix. Species containing alkali metals were produced by doping the sample with the appropriate metal chloride solution on the probe tip. All samples were commercially available (Sigma Corp.) and used without further purification. Instrumental conditions and the pulse sequence used to observe metastable decay have been provided earlier.[18] Briefly, ions were produced by bombardment with a 10-kV Cs^+ beam and injected during a period of 10 ms. This period was chosen to provide a sufficient signal-to-noise ratio for analyses and yet short enough to observe the decay of the pseudomolecular ion. The detection delay time was varied relative to the end of the ion production/injection pulse. Differential pumping maintained a pressure of 10^{-9} Torr in the analyzer region during the experiment while the sample was in place. A slight pressure increase was observed when the cesium gun was turned on. While performing the bracketing experiments, we observed the presence of neutral glycerol in the analyzer chamber, indicating that a flux of neutral compounds travels down the axis of the quadrupole rods into the analyzer cell during the experiment. The neutral species could produce collisionally activated dissociation (CAD) or collisional ejection of the ions. However, both processes operate on all ions and would more strongly affect smaller ions.

The procedure for the determination of the rate constants from the metastable decay curve of protonated α-cyclodextrin has been described.[18] The decay curve of the pseudomolecular peak was fitted by a combination of an exponentially decaying function and a constant using a commercially available program (Kaleidagraph). Decay rates were calculated from the exponential part of the curve. Alternatively, a pseudo-first-order behavior can be assumed by neglecting the constant part of the curve. This procedure preserved the order of the rates obtained with the first method but yielded values that were consistently lower by about 40%. Slow metastable decay reactions such as those found for sodium and potassium coordinated species could not be determined with certainty by using the first method due to the difficulty in obtaining the contribution of the constant function. Furthermore, species with relatively weakly bound cations, e.g., sodiated and potassiated species, undergo metal ion loss reactions that could not be properly monitored due to the low mass limitation (masses below m/z 50 are not detected in the broad band mode) of the instrument. This limitation is a consequence of slow digitizing rates in the current instrumental setup. This means that the total ion abundance could not be normalized as ions were lost to the low-mass regime. Therefore, care was taken to ensure that the total ion abundance remained constant during the observation time. We have shown that proper tuning produces relatively stable ion abundances for protonated species during the lifetime of the experiments and using both relative and absolute abundances produced nearly identical results for the protonated species. To calculate the rates, absolute abundances were used from spectra obtained with detect delays between 1 and 5 ms when the contribution of the exponential function was greatest. For consistency, values obtained using a pseudo-first-order decay were scaled to the first method by use of the values obtained for the protonated species. These values are listed in Table 1.

(29) McCullough, S. M.; Gard, E.; Lebrilla, C. B. *Int. J. Mass Spectrom. Ion Processes* **1991**, *107*, 91.

Table 1. Rate Constants for the Unimolecular Metastable Decay of α-Cyclodextrin and Maltohexaose Coordinated to Various Cations and Deprotonated α-Cyclodextrin Produced by LSIMS

	cation	rate const, s^{-1}	SD	detns
α-cyclodextrin	H	428	44	13
	Li	385	24	4
	Na	346	36	5
	K	240	25	3
maltohexaose	H	410	81	6
	Li	346	42	4
	Na	231	18	6
	K	252	28	4
α-cyclodextrin anion		193	22	9

[a] The standard deviation (SD) values were calculated from the multiple determinations.

RESULTS

Figure 1a (top) shows a typical spectrum of a cationized oligosaccharide accumulated from 100 scans with a 10-ms injection width and 1-ms detect delay. For purposes of observing the direct competition between decay rates of protonated and alkali metal coordinated oligosaccharides, it was necessary to obtain spectra which contained both species. This was performed by adjusting the concentration of the salt solution added to the sample in the matrix. A highly concentrated salt solution produced primarily the alkali metal coordinated species, while a dilute solution produced primarily protonated species. Increasing the detect delay time allows the cationized parents to dissociate before detection. The presence of both the protonated and the alkali metal coordinated oligosaccharide is illustrative. It shows directly the differing rates of metastable decay between the two cationized species. Similar competition experiments of protonated and potassiated α-cyclodextrin have been used as evidence for the existence of slow unimolecular processes.[18] The possibility of other ion loss mechanisms has been considered. Several processes are known for ion loss in FTMS, including collisional ejection, ion evaporation, and z-ejection.[30-32] These mechanisms, however, are nonmass specific and operate over a broad mass range. There are no known ion loss mechanisms that operate either on a specific mass or over a very narrow mass range. Furthermore, metastable decay is also observed with other compounds having different masses, including the maltohexaose discussed below and other linear oligosaccharides and peptides we have investigated in our group.

(30) Wang, M.; Marshall, A. G. *Anal. Chem.* **1990**, *62*, 515.
(31) Hanson, C. D.; Castro, M. E.; Kerley, E. L.; Russell, D. H. *Anal. Chem.* **1990**, *62*, 520.
(32) Caravatti, P.; Allemann, M. *Org. Mass Spectrom.* **1991**, *26*, 514.

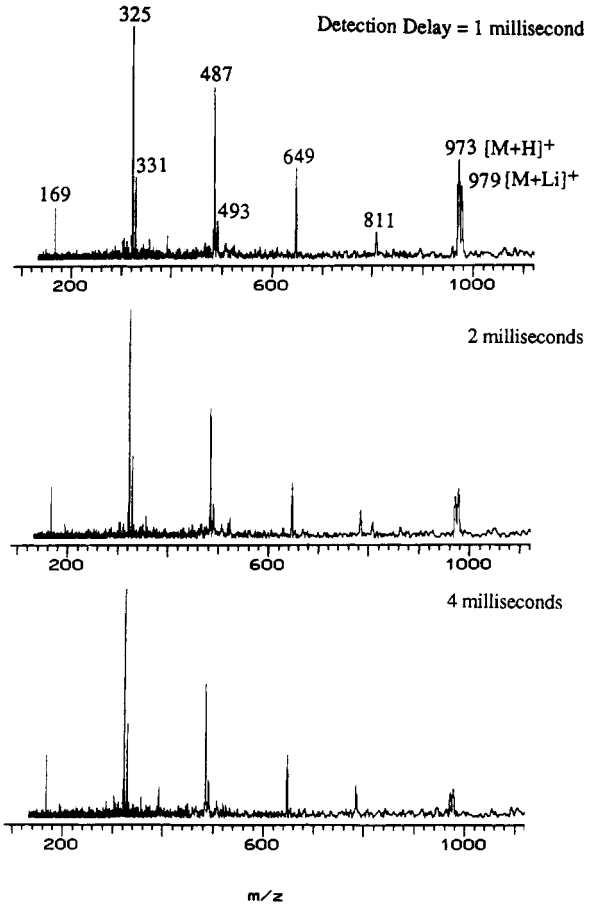

Figure 1. Spectra of α-cyclodextrin doped with an aqueous solution of LiCl produced from a glycerol/thioglycerol (1:1) matrix. The concentration was adjusted to provide strong abundances of both lithiated and protonated parents. Each spectrum is an accumulation of 100 scans using an injection width of 10 ms. The time indicated refers to the time between the end of the injection pulse and the beginning of the detect pulse.

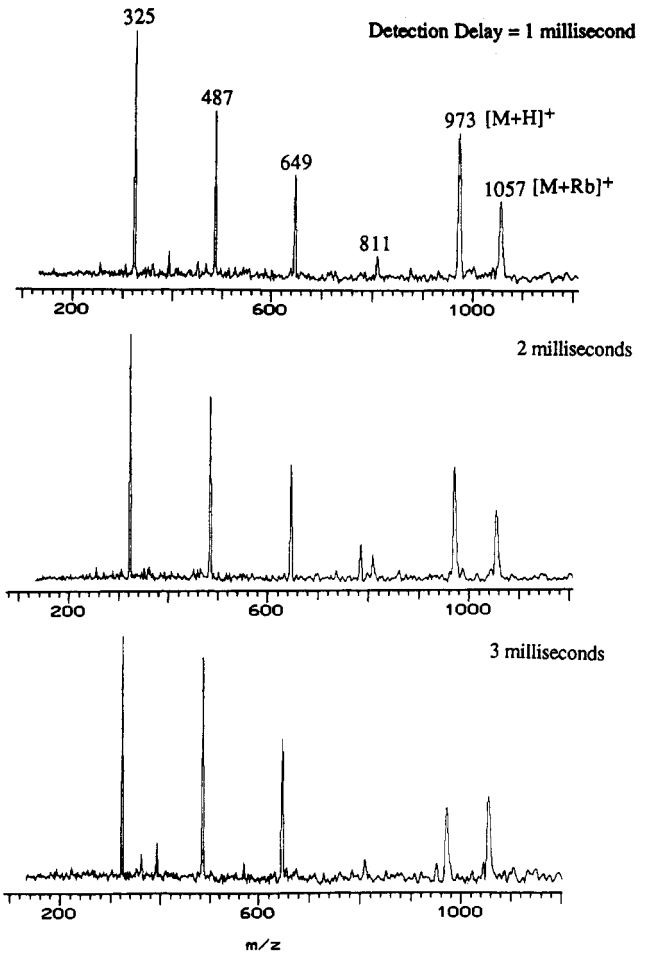

Figure 2. Spectra of α-cyclodextrin doped with an aqueous solution of RbCl produced from a glycerol/thioglycerol (1:1) matrix. The concentration was adjusted to provide strong abundances of both rubidium and proton coordinated parents. Each spectrum is an accumulation of 100 scans using an injection width of 10 ms. The time indicated refers to the time between the end of the injection pulse and the beginning of the detect pulse.

In all competition experiments involving alkali metal and proton coordinated α-cyclodextrin, we find that the protonated species decay with the fastest rates. The series of spectra shown in Figures 1 and 2 are representative of the competition experiments involving oligosaccharides coordinated to small (Li) and large (Rb) alkali metal ions. The fragment ions are derived more from the protonated species than the alkali metal coordinated species. In Figure 1 the intense pyran ion series having m/z 325, 487, 649, and 811 is consistent with the fragmentation pattern of protonated α-cyclodextrin. Fragment ions having m/z 169, 331 and 493 make up the lithium analog of this series. Larger fragments coordinated to lithium are not observed in this example as they are relatively less abundant than the smaller fragments. They are observed in spectra from samples containing higher concentrations of lithium salt, i.e., greater than a 1:3 molar ratio of LiCl to oligosaccharide. In these instances, even though the protonated species were observed to have slightly greater abundances at the shortest detection delay time, their intensities were found to decrease faster than any metal-containing species, so that after several milliseconds the metal-containing species became the more intense peak. Differences in the behavior of various metal cations are observed in the fragment ions present in the spectra. Lithiated and sodiated oligosaccharides decompose to produce the respective coordinated fragments. However, we generally find that the spectra of lithiated species contain more metal-coordinated fragments than sodiated species. Doping the sample with larger alkali metals including K, Rb, and Cs produced no fragments coordinated with metal ions. For example, in the series of rubidium spectra shown in Figure 2, all the fragments are derived strictly from the protonated parent.

The fragment ions in the LSIMS spectra are believed to originate from a combination of metastable decay and decomposition during direct ion bombardment (both in solution and in the gas phase). The lack of alkali metal containing fragments from samples doped with K^+, Cs^+, and Rb^+, however, indicates a single process in which all fragments are produced by metastable decay. Otherwise, fragment ions should contain some metal-containing species as observed with the parent ion. The generally weaker abundances of fragments containing alkali metal cations when present, compared to those containing protons in both Figures 1 and 2, indicate that the protonated parent was initially produced in significantly greater abundance than the alkali metal containing parent and that a large portion of the protonated species rapidly decomposed even before they could be detected.

The metastable decays of metal cationized oligosaccharides are best observed under high concentrations of the metal salt

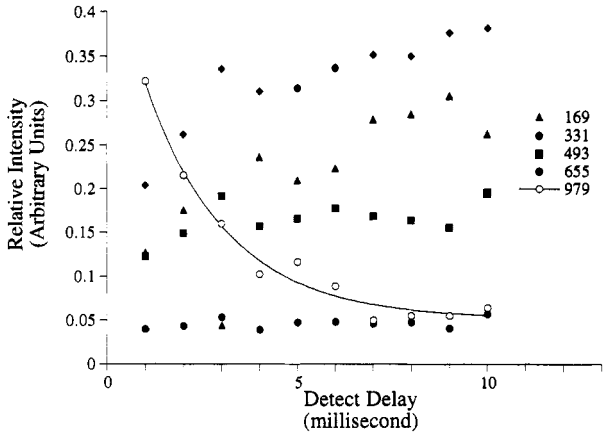

Figure 3. Relative abundances of lithiated α-cyclodextrin and its fragment ions as a function of detection delay times. The ion having m/z 979 (empty circles) is the lithium coordinated parent. All other ions are fragments coordinated to the lithium cation.

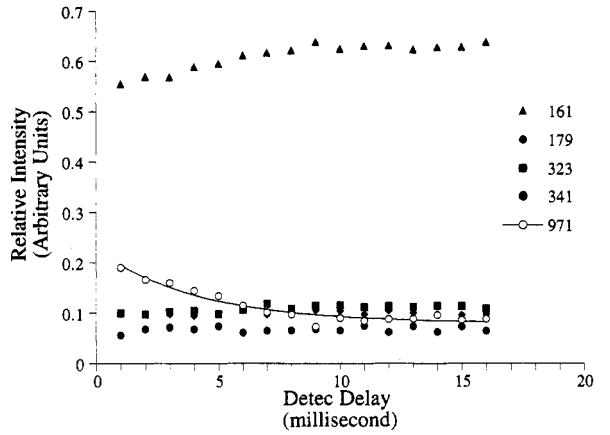

Figure 4. Relative abundances of deprotonated α-cyclodextrin and its fragment ions as a function of detection delay time. The ion having m/z 971 is the deprotonated parent. All other ions (filled points) are fragments of α-cyclodextrin.

producing parents coordinated to the respective metal cation. For example, spectra derived from a sample with significantly greater lithium chloride concentration show primarily the lithiated species near the molecular ion region with only minor abundances of the protonated parent. The time plot (Figure 3) shows a decay of the parent and a rise in small fragments, more notably m/z 169, 331, and 493 between 1 and 10 ms.

Several research groups have reported that lithiated species produce cross ring cleavages.[27,28,33] We observe similar behavior but not in the conditions under which these experiments were performed. Cross ring cleavages are often significantly less intense than glycosidic bond cleavage. The relatively poor signal-to-noise ratio produced during these experiments does not allow observation of these fragment ions.

Unimolecular decay of the anion (deprotonated) species is also observed (Figure 4). Fragmentation is characterized by the abundance of lower mass ions corresponding to mono- and disaccharide fragments. Cross ring fragmentation reactions are sometimes observed in the spectra of oligosaccharide anions but are not observed here. Inspection of the time plots shows that a rise in the intensity of m/z 161 accompanies the decay of the deprotonated parent. Large

(33) Grese, R. P.; Gross, M. L. *J. Am. Chem. Soc.* **1990**, *112*, 5098.

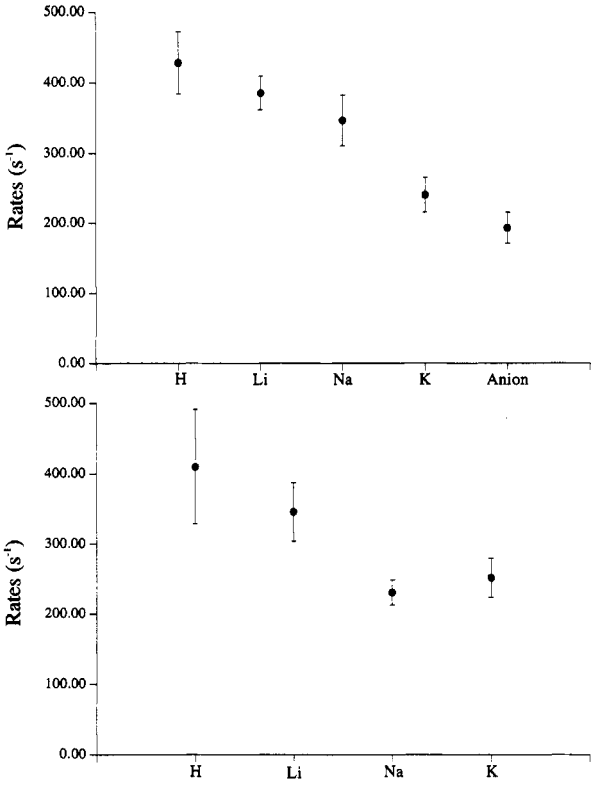

Figure 5. Graphical representation of the rate constants from Table 1 as a function of coordinating atom for (a, top) α-cyclodextrin and (b, bottom) maltohexaose. The error bars are represented by the vertical lines at each point.

fragment ions are not readily observed owing to the differences in the reaction mechanisms between cationic and anionic fragmentation. The fragmentation pattern of deprotonated α-cyclodextrin obtained by FTMS has been discussed in a recently published report.[34]

Rate constants for the unimolecular decay of cationized α-cyclodextrin and maltohexaose, its linear analog, are tabulated (Table 1). The relative standard deviations listed are calculated from the sets of multiple determinations. It should be noted that the rate constants are obtained from a population of ions injected during a 10-ms interval. During this time metastable decay is already occurring to the portion of ions which were trapped early in the injection period. The absolute values listed in Table 1, therefore, contain a degree of error and should be used either comparatively or to observe trends. The rate constants, however, reflect the result observed in the competition experiment, that is, the protonated species have the fastest metastable decay rate. Graphical representations of the results show clear trends in the decay of the various ionic species (Figure 5). In general, the protonated species have the fastest decay rates of any other ionic species. For cyclodextrin, the order of decay rates follows, $H^+ > Li^+ > Na^+ > K^+ >$ anion. The results for maltohexaose (18 mass units greater than α-cyclodextrin) are not as regular but the general trend is preserved, i.e., $H^+ > Li^+ > Na^+ \approx K^+$. Both protonated oligosaccharides have similar rates, although some variations are observed for specific alkali metals. The most noticeable difference between the two groups of ions is the

(34) Carroll, J.; Ngoka, L.; Beggs, C. G.; Lebrilla, C. B. *Anal. Chem.* **1993**, *65*, 1582.

relatively slower rate for sodium coordinated maltohexaose compared to the sodium coordinated α-cyclodextrin.

DISCUSSION

The fragmentation behavior of oligosaccharide cations and anions under the long time scale of the FTMS technique has been discussed in several earlier papers.[25,34,35] It is important to point out that the experimental conditions used to observe metastable decay differ from those used to perform analyses for structural elucidation. In contrast to the short injection times reported in this work, structural analyses are performed by optimizing fragmentation with long injection times (500 ms) and fewer scans.[10]

The ordering of the decay rates is consistent with earlier observations made in this and other laboratories. From the results presented, one may conclude that the different rates of metastable decay play a strong role in observed differences in sensitivity. Generally greater sensitivity is observed in FAB/FTMS when alkali metals are used as cations. We have observed, for example, that lithiated parents of oligosaccharides often persisted better than the analogous protonated parent at long detect delays. High-resolution analyses, which require longer observation times than the usual mass analyses, are easier to perform with lithiated oligosaccharides than with protonated oligosaccharides. Higher sensitivity brought about by cationization with alkali metal ions has long been known with sector instruments.[21,36] It is apparent that in sector instruments, as in FTMS instruments, a large portion of the protonated species may decompose before the ions are even detected.

At least two processes are thought to give rise to the observed spectra: (a) decomposition to cationized oligosaccharide fragments and (b) elimination of the alkali metal ions. The relative contributions of these two processes in turn invariably depend on the internal energy obtained during ionization and the ability of the cation to catalyze fragmentation. LSIMS ionization involves a combination of processes including desorption of preformed ions from solution- and gas-phase ionization not unlike that of chemical ionization.[37-39] Although the desorption processes remain technically difficult to characterize in terms of energy, the gas-phase processes can be modeled by ion/molecule reactions.

$$M + C^+ \rightleftharpoons MC^+ \quad \Delta H < 0 \qquad (1)$$

C = H, Li, Na, K, etc.

$$M + SC^+ \rightleftharpoons MC^+ + S \qquad (2)$$

S = matrix

Any gas-phase processes would inevitably involve the coordination of a proton or an alkali metal ion either directly in an exothermic reaction (reaction 1) or indirectly through cation exchange (reaction 2). Cation affinities ($-\Delta H$) are not known for oligosaccharides that contain a multitude of coordination sites. However, several reports provide clues to the relative cation affinities of oligosaccharides. "Cationizing efficiencies" have been measured by Roczko et al. in laser desorbed mono- and disaccharides.[40] Li^+ and Na^+ were found to be better than K^+, Rb^+, and Cs^+ in producing the coordinated species. Without providing actual cation affinities, Veith suggested using field desorption studies that the relative cation affinities of raffinose, a trisaccharide, follow the order $Cs^+ < K^+ < Na^+ < Li^+$.[41]

Table 2. Cation Affinities ($-\Delta H$, eq 1) of Ethylene Glycol and Its Dimethyl Ether for Various Cations Obtained by Bracketing Measurements

	$-\Delta H$, kcal/mol			
binding to	H^+	Li^+	Na^+	K^+
## IIa ##	196.0[a]	50.0 ± 5.4[b]	39.3 ± 5.9[b]	27.5 ± 1.5[b]
ethylene glycol dimethyl ether	204.9[c]	56.7[d]	47.2[e]	30.8[f]

[a] See ref 46. [b] Obtained from bracketing techniques. See ref 47. [c] See ref 48. [d] Obtained from the data in refs 49 and 50–52. [e] See refs 53 and 54. [f] See ref 55.

The relative magnitude of the binding can be approximated using compounds with known cation affinities which can bind alkali metals in ways similar to oligosaccharides (Table 2). As examples, both ethylene glycol and its dimethyl ether derivative contain hydroxyl and ether groups found in oligosaccharides. The exothermicity of cation binding to both compounds follows the order $H^+ > Li^+ > Na^+ > K^+$, similar to the order found by Veith. The most exothermic reaction, i.e., protonation, is also associated with the largest unimolecular rate constant. This suggests that protonated species are formed with greater energy, thereby facilitating fragmentation.

The size of the cation may somewhat affect the ordering of the alkali metal ions in the oligosaccharides. The large number of hydroxyl groups could favor larger cations producing greater stabilization. However, the presence (or absence) of cations bound to oligosaccharide fragments reflects the trend in cation affinities found in Table 2. The proton is naturally found in all fragments produced from the protonated parent. Lithiated fragments are also observed more commonly than sodiated fragments. Fragment ions coordinated to K^+, Cs^+, and Rb^+ are not observed, reflecting the propensity of these respective species to lose the cations during decomposition. The inverse correlation between the decay rates and cation affinity is not necessarily a strong one. The proton affinities of both model compounds are nearly 150 kcal/mol greater than the affinities for any alkali metal ions. By contrast, the affinities for the alkali metal ions decrease progressively with increasing size by only about 10 kcal/mol. This would mean that the decay rate of the protonated species should be significantly faster than all the metal cationized species. Instead, the difference in the rates between protonated and lithiated species is nearly the same as that between lithiated and sodiated species. The discrepancy points to the complexity of LSIMS ionization and the contribution of gas-phase cation-transfer reactions represented by reaction 2. The latter is

(35) Carroll, J. A.; Lebrilla, C. B. *Org. Mass Spectrom.* **1992**, *27*, 639.
(36) Puzo, G.; Prome, J. C. *Org. Mass Spectrom.* **1985**, *20*, 288.
(37) Pachuta, S. J.; Cooks, R. G. *Chem. Rev.* **1987**, *87*, 647.
(38) Sunner, J.; Morales, A.; Kebarle, P. *Anal. Chem.* **1988**, *60*, 98.
(39) Williams, D. H.; Findeis, A. F.; Naylor, S.; Gibson, B. W. *J. Am. Chem. Soc.* **1987**, *109*, 1980.
(40) Roczko, A. W.; Viswanadham, S. K.; Sharkey, A. G.; Hercules, D. M. *Fesenius Z. Anal. Chem.* **1989**, *334*, 521.
(41) Veith, H. J. *Tetrahedron* **1977**, *33*, 2825.

Scheme 1. Commonly Proposed Gas-Phase Fragmentation Reactions of Protonated and Deprotonated Oligosaccharides

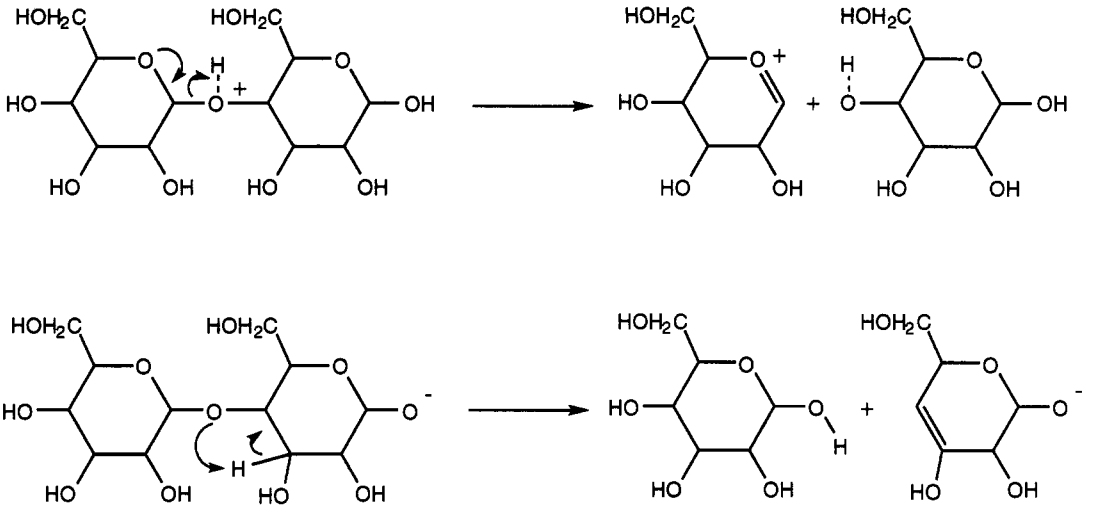

further illustrated by the transfer reaction involving ethylene glycol (EG) its dimethyl derivative (EGDE, reaction 3). This reaction is generally exothermic, but the differences in the heats of reactions are considerably less than the cation binding reactions represented by reaction 1. For reaction 3 the following heats of reactions are obtained for the respective cations: 8.9 (H^+), 6.7 (Li^+), 7.9 (Na^+), and 3.3 kcal/mol (K^+).

$$EG\cdots C^+ + EGDE \rightleftharpoons EG + EGDE\cdots C^+ \qquad (3)$$

EG = ethylene glycol; EGDE = ethylene glycol dimethyl ether; C = H, Li, Na, K, etc.

The ability of the cation to promote bond cleavage also favors the facile fragmentation of protonated oligosaccharides. The fragmentation of protonated species involves primarily cleavage along glycosidic bonds whereas fragmentation of metal-containing species and anionic species includes more complex, multiple cleavage reactions.[27] The major fragmentation reaction of protonated oligosaccharides, shown in Scheme 1 for a disaccharide, produces a relatively stable oxonium ion and a neutral monosaccharide. An analogous reaction involving a metal cation would be unfavorable, producing a gas-phase alkoxide salt (e.g., Li^+OR^-). It is more likely that fragmentation reactions of these metal-coordinated species proceed by a manner similar to anionic ones in which the charge behaves more or less as a spectator. Indeed, the comparison of the fragments from lithium cationized and anionic oligosaccharides shows fragment ions which appear to come from similar reactions.[34] There are several experiments which support the relatively high reactivity of protonated species to fragmentation.[42] From the investigation of amino sugars, Martin et al. concluded that laser desorbed oligosaccharides of MNa^+ ions fragment "somewhat easier" than MK^+ ions.[43] Similarly, they observed that in plasma desorption spectra where both MH^+ and MNa^+ ions are formed, fragment ions are primarily from glycosidic bond cleavage from MH^+ even though MNa^+ ions predominate. Furthermore, glycolipids, when protonated can undergo unfavorable, high-energy cleavages that are not observed with the sodiated parents.[21]

Chart 1. Representation of the Bond Lengthening Behavior of Protonated Glucose and Methylated Glucose, Calculated by a Semiempirical (AM1) Molecular Orbital Method

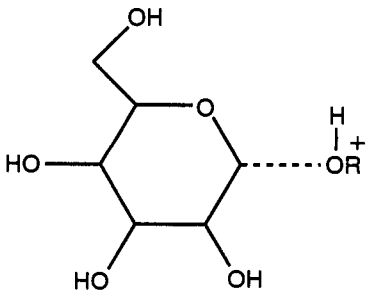

R = H, CH_3

Calculations have been performed in our group dealing with the effects of protonation of various sites on fragmentation reactions.[44] The semiempirical molecular orbital calculations (AM1) of protonated glucose structures predict that the anomeric oxygen is not necessarily the most basic position. Intramolecular interactions, specifically with neighboring hydroxyl groups, strongly determine the basicity of individual sites. Proton affinities of the various sites vary by as much as 7 kcal/mol. However, protonation of the anomeric oxygen (Chart 1) causes a lengthening of the C–O bond from 1.4 to nearly 3.0 Å when R = H or CH_3 to produce a loose ion/dipole complex involving an H_2O, or CH_3OH, coordinated to an oxonium ion. In other words, cleavage of the glycosidic bond may not require overcoming a reaction barrier but simply the interaction of a relatively weak ion/dipole complex. Replacing the methyl group with a saccharide unit, a larger alkyl group, is not expected to greatly change this result.

The relatively slow decay rate of the anion compared to the cations is intriguing but consistent with the persistence of the deprotonated signal commonly obtained in anion spectra. Gas-phase acidities of complex compounds are even less available than gas-phase basicities, making comparison of energetics involving deprotonation and protonation reactions

(42) Laine, R. A.; K. M. P.; French, A. D.; Hall, R. W.; Abbas, S. A.; Jain, R. K.; Matta, K. L. *J. Am. Chem. Soc.* **1988**, *110*, 6931.
(43) Martin, W. B.; Silly, L.; Murphy, C. M.; T. J. Raley, J.; Cotter, R. J. *Int. J. Mass Spectrom. Ion Processes* **1989**, *92*, 243.
(44) Willard, D.; Carroll, J.; Lebrilla, C. B., unpublished results.

neither possible nor appropriate. Fragmentation reactions of the anion are generally believed to proceed through several steps, unlike the single-step proton-catalyzed glycosidic bond cleavages. If, for example, the anionic cleavage of glycosidic bonds (Scheme 1) does not involve the charge, then it may occur over activation barriers not unlike those found in analogous neutral reactions. The relatively slower rate of the anionic species is an indication that cations do induce fragmentation, albeit in varying degrees. The preference for smaller ionic products in the positive ion mode is presumably because large fragment ions have sufficient internal energy to further decompose. This preference is observed in nearly all metastable reactions including those of the lithiated species (Figure 3).

The decay rates for the large biomolecules produced by LSIMS are comparable to reported radiative association rates, thereby giving these vibrationally excited molecules another mode of relaxation. Radiative rates of 0.98×10^2 s^{-1} have been reported for the proton bound dimer of acetone produced by collisional association.[45] It is not clear how radiative relaxation would affect the ordering of the metastable rates since little is known about the process. However, there are no compelling reasons to believe that radiative rates will differ for individual cationized species, unless differences in binding energy will somehow affect radiative rates. In any case, further discussions would only be speculative at this point. It would be useful to know whether radiative association is size dependent.

The results generally suggest the effectiveness of various cations and the charge state for analyses. Protons coordinate strongly but produce only one type of cleavage and often weakly abundant pseudomolecular ions. Fragmentation reactions, both during ionization and under CAD conditions, occur more commonly with protonated species. Alkali metal coordinated species produce cross ring cleavage but are limited in effectiveness by the relatively weaker binding energy. When the results presented here are combined with those from other studies involving rare earths and transition metals, it is apparent that lithium and possibly sodium are best for analyses.[26,36] These metals coordinate to produce abundant pseudomolecular ions which dissociate to yield structurally important fragment ions. Larger alkali metals are not as useful because the coordinated species primarily lose the metal cations during fragmentation.

(45) Kofel, P.; McMahon, T. B. *J. Phys. Chem.* **1988**, *92*, 6174.
(46) Bouchoux, G.; Jezequel, S.; Penaud-Berruyer, F. *Org. Mass Spectrom.* **1993**, *28*, 421.
(47) Gal, J. F.; Lebrilla, C. B., unpublished results.
(48) Lias, S. G.; Liebman, J. F.; Levin, R. D. *J. Phys. Chem. Ref. Data* **1984**, *13*, 695.
(49) Taft, R. W.; Anvia, F.; Gal, J.-F.; Walsh, S.; Capon, M.; Holmes, M. C.; Hosn, K.; Oloumi, G.; Vasanwala, R.; Yazdani, S. *Pure Appl. Chem.* **1990**, *62*, 17.
(50) Woodin, R. L.; Beauchamp, J. L. *Chem. Phys.* **1979**, *41*, 1.
(51) Staley, R. H.; Beauchamp, J. L. *J. Am. Chem. Soc.* **1975**, *97*, 5920.
(52) Woodin, R. L.; Beauchamp, J. L. *J. Am. Chem. Soc.* **1978**, *100*, 501.
(53) Keesee, R. G.; Castleman, A. W. *J. Phys. Chem. Ref. Data* **1986**, *15*, 1011.
(54) Maria, P. C.; Taft, R. W., unpublished results.
(55) Sunner, J.; Kebarle, P. *J. Am. Chem. Soc.* **1984**, *106*, 6135.

ACKNOWLEDGMENT

Funds provided by the National Institute of General Medical Sciences (NIH GM49077-01), is gratefully acknowledged. J.F.G. thanks the Région Provence-Alpes-Cote d'Azur Council for the travel grant to UC Davis.

Received for review September 7, 1993. Accepted December 1, 1993.[⊗]

[⊗] Abstract published in *Advance ACS Abstracts*, January 15, 1994.